

# Use of Amide Exchange Mass Spectrometry To Study Conformational Changes within the Endopolygalacturonase II–Homogalacturonan–Polygalacturonase Inhibiting Protein System<sup>†</sup>

Daniel King,<sup>‡</sup> Carl Bergmann,<sup>‡</sup> Ron Orlando,<sup>\*,‡</sup> Jacques A. E. Benen,<sup>§</sup> Harry C. M. Kester,<sup>§</sup> and Jaap Visser<sup>§</sup>

Complex Carbohydrate Research Center, Department of Chemistry, University of Georgia, 220 Riverbend Road, Athens, Georgia 30602-4712, and Section of Molecular Genetics of Industrial Microorganisms, Wageningen Agricultural University, Wageningen, The Netherlands

Received February 12, 2002; Revised Manuscript Received May 30, 2002

**ABSTRACT:** Amide exchange mass spectrometry (MS) was used to study the enzyme endopolygalacturonase II (EPG-II) from *Aspergillus niger* as it binds to an oligosaccharide substrate. A localized decrease in the level of deuterium incorporation in EPG-II of the EPG-II–oligosaccharide complex relative to that of the free EPG-II identified the location of substrate contact, which is in agreement with published site specific mutation studies. In addition, when bound with substrate, regions of EPG-II remote from the substrate binding site became exposed to the solvent, as revealed by an increase in the amount of incorporated deuterium, indicating a conformational change in the enzyme. Fluorescence experiments were performed to provide additional evidence for an altered conformation of EPG-II as a result of substrate binding. This novel application of amide exchange-MS to the study of protein–carbohydrate binding has, for the first time, described in detail the conformational changes associated with EPG-II when it binds a substrate. Amide exchange-MS was also used to study the interactions of EPG-II and the polygalacturonase inhibitor protein (PGIP). Mass spectral data of the EPG-II–oligosaccharide complex in the presence of *Phaseolus vulgaris* PGIP indicate that the inhibitor contacts EPG-II at a site remote from the substrate binding cleft, and is restricting the conformational changes of EPG-II. Fluorescence experiments also revealed that upon binding of PGIP, the conformational changes mentioned above for the EPG-II–substrate complex are minimized. These results, together with previously reported data, point to a location on EPG-II for interaction with PGIP as well as a possible mechanism for noncompetitive inhibition of EPG-II.

A major goal of plant pathogenesis research is the thorough characterization and understanding of the interactions between pathogen-derived plant cell wall-degrading enzymes and plant cell wall carbohydrate substrates. Plant cell walls are composed of two interacting networks, a cellulose/hemicellulose network and a pectin network (1). The pectin network includes several related acidic polysaccharides such as rhamnogalacturonan-I (RG-I), rhamnogalacturonan-II (RG-II), and homogalacturonan, also known as polygalacturonic acid (PGA)<sup>1</sup> (2). Pectins form a major component of the primary cell walls of dicotyledons and nongraminaceous monocotyledons and are found at high concentrations in the middle lamella (3). Among the microbial phytopathogens are viruses, bacteria, and fungi. Fungi often gain entry into the plant via the cell wall, often through the middle lamella (4). Endopolygalacturonases (EPGs) are a major

component of the pectin-degrading activity of phytopathogenic fungi and are among the first degradative enzymes to be secreted upon fungal infection (5, 6). EPGs hydrolyze deesterified regions of wall-bound homogalacturonans, solubilizing RG-I and RG-II, and open the wall to the action of other exo- and endoglycanases, including cellulases, glucanases, xyloglucanases, and arabinoxylanases (3, 7).

During pathogenesis, there is a potential for interaction between EPGs and plant cell wall-derived EPG inhibitors known as polygalacturonase inhibiting proteins (PGIPs) (3, 8). PGIPs are soluble, leucine rich repeat (LRR) glycoproteins, found in the cell wall (9). PGIPs form high-affinity complexes with EPGs in a reversible, stoichiometric manner. The rate of hydrolysis of homogalacturonan by an EPG–PGIP complex is, depending on the source of the EPG and PGIP, between 1 and 2 orders of magnitude slower than that of the free EPG (10). The inhibition of EPGs by PGIPs not only may slow the gross action of EPGs on the solubilization and fragmentation of homogalacturonan but also will extend the lifetime of biologically active oligogalacturonides (fragments of homogalacturonan) released from the cell wall by the action of EPGs. Since oligogalacturonides have been implicated in the defense response of plants, extending their lifetime likely contributes to a successful defense response (5, 6, 10, 11).

<sup>†</sup> We acknowledge and are grateful for financial support of this research provided by the National Institutes of Health (NIH Grant P41RR05351), the North Atlantic Treaty Organization (NATO Grant CRG973086), the Department of Energy (DOE Grants DE-FG02-93ER20097 and DE-FG02-96ER20221), and the National Science Foundation (NSF Grant MCB-0115132).

<sup>‡</sup> University of Georgia.

<sup>§</sup> Wageningen Agricultural University.

<sup>1</sup> Abbreviations: RG, rhamnogalacturonase; PGA, polygalacturonic acid; EPG, endopolygalacturonase; PGIP, polygalacturonase-inhibiting protein; LRR, leucine rich repeat; MS, mass spectrometry.

EPGs from a single strain of fungus may exist in a variety of isoforms, each of which may consist of a series of glycoforms. There is evidence that the heterogeneity among the EPGs allows for variability in their mode of action as well as in their ability to interact with, and be inhibited by, PGIPs (11, 12). In addition, the PGIPs of a single plant species may also be present as a set of isoforms and their associated glycoforms (ref 13 and unpublished data of this lab). This isoform–glycoform variability provides the potential for a wide spectrum of specificity of EPG–PGIP interactions within any plant–pathogen pairing. There are a number of examples in which different EPG–PGIP pairings demonstrate different degrees of inhibition. Additionally, both competitive and noncompetitive types of inhibition have been reported. Such data indicate that the location of interaction may differ and is, at least in some cases, not at the active site (14). The mode of action of a particular fungal EPG and its inhibition by PGIPs may be critical factors in determining whether the fungus is a viable pathogen.

A proposed model for the structure of a bean PGIP, based on its membership in the plant specific LRR class of proteins, has recently been published (15). In addition, site specific mutation experiments indicate a role for several specific amino acids within the PGIP during a fungal EPG–PGIP interaction (16). A recent study identified sites of nine amino acids in PGIPs and nine amino acids in EPGs that are likely candidates for natural mutation, thus altering the specificity of interaction of the two proteins (17). This study supported the conclusions from the site specific mutation experiments mentioned above (16), but also indicated other regions on the PGIP which may be important for binding to EPGs.

Crystal structures for a bacterial (18) and a fungal EPG (19) have been determined and serve as a model for EPGs. All EPGs are members of family 28 of the glycosyl hydrolases, as classified by the Henrissat structural classification scheme (20); thus, it is not surprising that the overall structure of the bacterial EPG resembles that of the fungal EPG. Despite these similarities, PGIPs inhibit fungal EPGs but do not inhibit bacterial EPGs. To date, no complete model of the EPG–PGIP complex has been proposed. Due to the difficulty in cocrystallizing two relatively large proteins of approximately 35 000 Da each, both of which show heterogeneity of glycosylation, it is unlikely that a crystal structure of the complex will be available soon.

The degradation of plant cell walls plays a significant role in both the ripening and rotting of fruits and vegetables. The importance, both agriculturally and commercially, of the action of EPGs on pectin has led to a large body of research that attempts to fully understand, and thus exploit, EPGs (21–23). Agricultural communities, interested in prolonging the lifetime of crops, are concerned about inhibiting EPG activity (24). On the other hand, there are many industrial uses for an enzyme capable of degrading plant cell walls. For example, EPGs are used in the clarification of fruit juices, in the removal of color from paper, and in detergents to improve the removal of stains (22, 25).

We have begun to study the EPG–homogalacturonan interaction using mass spectrometry coupled with amide hydrogen–deuterium exchange. Amide exchange–MS monitors the rate at which amide hydrogens on a protein backbone exchange with hydrogen or deuterium in the solvent. Amide hydrogens are labile and will freely exchange with the

protons in solution if they are on the exterior of the protein, accessible to the solvent. When a protein is immersed in D<sub>2</sub>O or a mixture of D<sub>2</sub>O and H<sub>2</sub>O, amide hydrogens will be replaced with deuterons, each resulting in a mass increase of 1 Da, a change easily monitored by mass spectrometry (26–28).

In a recent variation of amide exchange–MS, the protein is enzymatically digested to determine specifically where deuterium is being incorporated (29–31). Typically, after <1 min, at neutral pH, all exterior amide hydrogens will be able to exchange with deuterium in the solvent. The protein is then digested, and the peptides are evaluated. The deuterium exchange must therefore be quenched to prevent both new deuterium from being added to interior amino acids exposed as a result of digestion and back exchange of the deuterium during the LC–MS process. The amide hydrogen–deuterium exchange rate decreases with temperature and pH (minimum at ~2.5). By placing the system in an ice bath and lowering the pH to 2.5, one can extend the half-life time of the deuterium on the protein to 40–50 min (32). Therefore, any changes within the binding of the system due to the quenching conditions will not have a significant effect on the deuterium incorporation levels as the exchange rates are slow during this time. The extended half-life times are typically long enough to allow for enzymatic digestion and LC–MS analysis (33, 34). Pepsin is used for proteolytic digestion because its optimal activity is at low pH. To study protein–substrate binding, a protein is analyzed in the presence and absence of a substrate. The substrate will protect exterior amino acids from deuterium incorporation in the region of its interaction. This approach has been used previously to investigate sites of protein–protein and protein–ligand interactions (29–31).

In addition to analysis of the enzyme–substrate complex, amide exchange–MS was also used to describe the structure of the *Aspergillus niger* EPG–*Phaseolus vulgaris* PGIP complex, as well as provide insight into the mechanism of inhibition. Using the methods developed here, other EPG–PGIP complexes with different attributes may be studied in the future as a means of understanding the variations in EPG–PGIP interactions and the possible role of this protein–protein interaction in pathogenicity.

## MATERIALS AND METHODS

**Materials.** Pepsin and D<sub>2</sub>O were purchased from Sigma (St. Louis, MO). The D201E mutant form of EPG-II was prepared as published (hereafter denoted as mEPG-II) (35). The octamer of galacturonic acid [(GalA)<sub>8</sub>] was a kind gift from S. Eberhard at the Complex Carbohydrate Research Center. *P. vulgaris* PGIP was prepared as described previously (36). Recombinant PGIP-II was a kind gift from F. Cervone (University of Rome “La Sapienza”, Rome, Italy). Acetic acid from J. T. Baker (Phillipsburgh, NJ) and acetonitrile from Fisher Scientific (Pittsburgh, PA) were used to prepare the LC buffers. Buffer A consists of 94% H<sub>2</sub>O and 6% acetic acid (v/v). Buffer B consists of 77% acetonitrile, 17% H<sub>2</sub>O, and 6% acetic acid.

**Amide Exchange–MS.** A total of four types of experiments were performed: mEPG-II in H<sub>2</sub>O (1), mEPG-II in 50% D<sub>2</sub>O (2), mEPG-II bound with (GalA)<sub>8</sub> in 50% D<sub>2</sub>O (3), and mEPG-II bound with PGIP and then incubated with (GalA)<sub>8</sub>

in 50% D<sub>2</sub>O (4). The mutant EPG-II stock was 1 mg/mL, and 10  $\mu$ L aliquots were placed into four microcentrifuge tubes. An equimolar amount of PGIP was added to tube 4, and 10  $\mu$ L of distilled water was added to tubes 1–3 as a blank. All four tubes were incubated at room temperature overnight to ensure mEPG-II–PGIP interaction. Next, a 100-fold molar excess of (GalA)<sub>8</sub> was added to tubes 3 and 4, and all four tubes were incubated at room temperature for 24 h. Subsequently, 20  $\mu$ L of H<sub>2</sub>O was added to tube 1, and 20  $\mu$ L of D<sub>2</sub>O was added to tubes 2–4 to attain an approximately 50% D<sub>2</sub>O concentration. The samples were left to exchange for a further 24 h. At the end of the incubation, the exchange was quenched by cooling the sample and lowering the pH. The tubes were placed in an ice bath, and 4  $\mu$ L of 0.1 M HCl was added to each tube to attain a final pH of 2.0. Four microliters of 1 mg/mL pepsin was then added, and the digestion progressed for 6 min. The solution was then analyzed by HPLC–MS.

To ensure against any back exchange of the deuterium, an ice bath was constructed to house the injection loop and reverse-phase HPLC column (25 mm long, 50  $\mu$ m MAGIC C18 Bullet, Michrom Bioresources, Inc., Auburn, CA). A Micromass Q-ToF-II (Manchester, U.K.), an electrospray ionization mass spectrometer, was used to record mass spectra continuously during the LC gradient program, which ran linearly from 20 to 65% buffer B over the course of 8 min. This instrumental configuration was previously determined to yield only minimal back exchange using this experimental protocol (37).

**UV Fluorescence.** Emission spectra were generated for free mEPG-II (1), mEPG-II in the presence of (GalA)<sub>8</sub> (2), and the mEPG-II–PGIP complex in the presence of (GalA)<sub>8</sub> (3) using a Shimadzu RF-5301 PC spectrofluorophotometer. Three 30 nM samples of mEPG-II were prepared. An equimolar amount of PGIP was added to sample 3 and the mixture allowed to incubate overnight. A 100-fold molar excess of (GalA)<sub>8</sub> was added to samples 2 and 3. All samples were then left at room temperature for 24 h. The samples were excited at 290 nm, and their emission maxima were recorded between 293 and 294 nm.

**BIAcore.** PGIP was immobilized on a BIAcore 3000 Chip following standard protocols provided by the manufacturer. After immobilization, EPG-II samples were passed across the chip. First, the BIAcore chip was exposed to the wild-type EPG-II, and binding of EPG-II to PGIP was detected by surface plasmon resonance (SPR). Then in a similar manner, mEPG-II was passed across the PGIP-immobilized chip and the SPR signals were compared.

## RESULTS AND DISCUSSION

**EPG-II–Homogalacturonan Interaction.** The use of pectin-degrading enzymes (PDEs) for industrial purposes has heightened the interest in understanding the interactions between the PDEs released by pathogens and plant cell wall carbohydrates. The polygalacturonases from various plant pathogens of both fungal and bacterial origin share regions of significant amino acid and structural homology. The X-ray crystal structures of EPG from the bacterium *Erwinia carotovora* and of EPG-II from the fungus *A. niger* have been determined (18, 19). The  $\beta$ -barrel structure found within EPG-II is very similar to that found in the crystal structures

determined in the past for pectate lyases that, for some time, have served as a model for the pectin-degrading enzymes (6). The prominent cleft along the barrel suggests a location for substrate binding in the active site. Site specific mutation experiments have been performed in an attempt to locate the key amino acids of the active site. Aided by homology searches, the mutation experiments identified several amino acids that are important for substrate binding and hydrolysis (35). Despite these advances, there are many questions that remain regarding the mechanism of hydrolysis of homogalacturonan by EPGs. The study of PDE–carbohydrate interactions has proven to be difficult if not impossible by traditional techniques. Therefore, the adaptation of amide exchange-MS to study the binding of EPGs with homogalacturonan seemed highly appropriate, due to the recent success of amide exchange-MS in studying protein–protein interactions (30–32, 38).

The enzyme EPG-II from the fungus *A. niger* was chosen for the initial experiments because of the availability of an EPG-II inhibitor protein, a mutant form of EPG-II, and a crystal structure for EPG-II. A number of concerns regarding the enzyme's compatibility with amide exchange-MS were encountered and will be discussed here, as many of these concerns will apply to future studies of other PDEs. EPG-II is a hydrolase, and as a result will not remain bound to the oligomeric substrate for the duration of the experiment. It was therefore necessary for a mutant of EPG-II to be prepared that maintained the binding capability without the hydrolytic activity. A number of mutants had been previously prepared and analyzed for activity and binding, and the D201E mutant was selected for having a  $K_m$  approximately equal to that of the wild type while showing negligible hydrolytic activity (35). Preliminary fluorescence (discussed later) and BIAcore experiments (results not shown) revealed that the D201E mutant has binding properties similar to those of the wild type and further support the appropriateness of this mutant for the experiments described herein. A second concern is that the active pH range for EPG-II lies between pH 4 and 5, far off the optimal pH of 7.0 for amide hydrogen–deuterium exchange experiments. The sample must therefore be allowed to exchange for more than the few minutes typically required of pH neutral protocols because exchange rates decrease with a decrease in pH, with a minimum exchange rate at pH  $\sim$ 2.5. Finally, a large percent of the protein, including the entire active site cleft, consists of  $\beta$ -pleated sheets which further decreases the rate of amide exchange for many amino acids (32, 39). Internal hydrogen bonding between pleated sheets makes it unlikely that much deuterium incorporation will occur in this region. However, as will be seen, the large degree of internal hydrogen bonding within pleated sheets proved to be advantageous.

Work has been published describing the activity of EPG-II with its natural substrate, polymeric homogalacturonan (40). The octamer of homogalacturonan, (GalA)<sub>8</sub>, was selected as the substrate in this study because modeling indicated it would be approximately the length of the cleft in EPG-II. A substrate that is too long might provide nonspecific protection to amino acids on sites outside the cleft, while a substrate that is too short would not indicate how much of the cleft is occupied by the substrate and may not participate in binding representative of homogalacturonan. The length of (GalA)<sub>8</sub> was estimated using the crystal



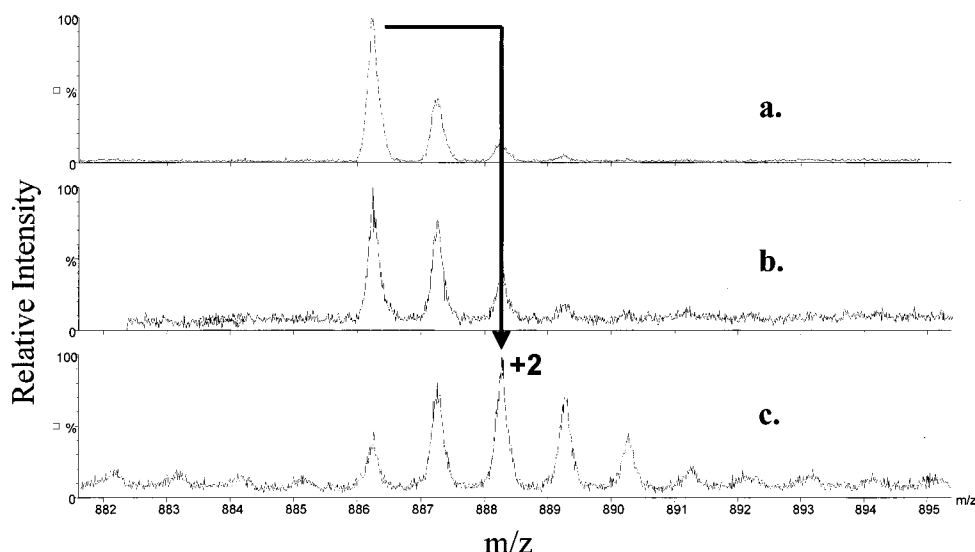


FIGURE 1: Mass spectra of a peptide (residues 131–139) from mEPG-II (a) in  $\text{H}_2\text{O}$ , (b) in  $\text{D}_2\text{O}$ , and (c) in the presence of a substrate in  $\text{D}_2\text{O}$ .

structures of other octamer oligosaccharides. The octamer of chitin [(GlcNAc)<sub>8</sub>], published by Papanikolaou et al. (41), was approximately 36 Å in length, and a tetramer of galacturonic acid [(GalA)<sub>4</sub>], published by Scavetta et al. (42), was approximately 17 Å in length.

To study EPG-II–homogalacturonan binding, three experiments were performed: mEPG-II in  $\text{H}_2\text{O}$  (control), mEPG-II in 50%  $\text{D}_2\text{O}$ , and mEPG-II in the presence of (GalA)<sub>8</sub> in 50%  $\text{D}_2\text{O}$  following the procedure presented in detail elsewhere (37). The deuterium exchange was quenched by reducing the temperature and pH. The mEPG-II samples were digested with pepsin, and the peptides were separated and detected by LC–MS. The peptides from the control trial were identified by matching their masses to those of a computer-generated peptic digest of mEPG-II, and only those yielding unambiguous matches were used for analysis. Pepsin was observed to consistently cleave most hydrophobic residues, in agreement with other reports (30, 43). The amount of deuterium incorporation into each peptide was then determined by comparing the spectra of the deuterated trials in the presence and absence of substrate (Figure 1). Figure 1a shows a singly charged peptide with a mass/charge ratio ( $m/z$ ) of 886. Figure 1b has the same isotope pattern, indicating a nondetectable amount of deuterium was incorporated into this peptide when the free mEPG-II was incubated in  $\text{D}_2\text{O}$ . A shift of the most abundant isotope peak can be used as an estimate of the mean deuterium incorporation for a peptide (32, 43), and Figure 1c shows such a change in the standard isotope pattern. The most abundant isotope increased by 2, indicating that the mean level of deuterium incorporation was approximately 2 deuterons. After evaluating the amide exchange–MS data, identifying the peptide, and estimating the amount of deuterium incorporation into each, we constructed a map of deuterium incorporation throughout the protein. The percent of deuterium incorporation was determined for small segments of mEPG-II. Figure 2a presents the changes in percent deuterium incorporation in short segments of mEPG-II caused by the presence of the substrate. There were three regions of the protein that underwent interesting changes in deuterium incorporation: the binding cleft, an  $\alpha$ -helix from Asp<sub>110</sub> to

Trp<sub>114</sub>, and the  $\beta$ -sheets on the underside of the  $\beta$ -barrel (Figure 3). Deuterium incorporation into peptides in the cleft area with and without the substrate indicated that the few residues that had been deuterated were protected from exchange by the presence of the oligosaccharide (Figure 3a). It is interesting to note that the distance between the most N- and C-terminal protected residues (Gly<sub>65</sub> and Tyr<sub>283</sub>) is similar to the length of the (GalA)<sub>8</sub> substrate. Gly<sub>65</sub> and Tyr<sub>283</sub> are approximately 38 Å apart in the EPG-II crystal structure, suggesting that the substrate lies somewhat linearly along the entire cleft.

For free mEPG-II, deuterium was incorporated somewhat unexpectedly into an  $\alpha$ -helix around Asp<sub>110</sub> (Figure 3a), although it is well documented that like  $\beta$ -pleated sheets,  $\alpha$ -helices are slow to incorporate deuterium due to the presence of hydrogen bonding (44, 45). These data imply that in the absence of substrate the  $\alpha$ -helix is either very loosely formed or not present at all, which contradicts the X-ray data. A loose  $\alpha$ -helix may become more structured during the crystallization protocol, emphasizing the need for developing techniques complementary to X-ray crystallography. Just as unexpected as the incorporation into this  $\alpha$ -helix was the apparent protection of the  $\alpha$ -helix by the substrate (Figure 3a). The helix is clearly located on the outside of the  $\beta$ -barrel and should not be directly protected by the substrate. Therefore, it is reasonable to suggest that a conformational change in mEPG-II upon substrate binding is responsible for the protection. There appear to be two possible causes for the indirect protection by the oligosaccharide; either the  $\alpha$ -helix is pulled into the interior of the protein, or the very loose  $\alpha$ -helix becomes more structured and the resulting increased level of hydrogen bonding within the helix prevents the exchange.

Due to the high percentage of hydrogen bonding ( $\beta$ -pleated sheets) within the protein, the majority of the peptides that were identified were from these regions and did not incorporate a detectable level of deuterium. Surprisingly, when mEPG-II was bound to the substrate, deuterium was incorporated into the  $\beta$ -sheets on the underside of the  $\beta$ -barrel (Figure 3b), implying a conformational change, most likely the disruption of these sheets. The detection of a local

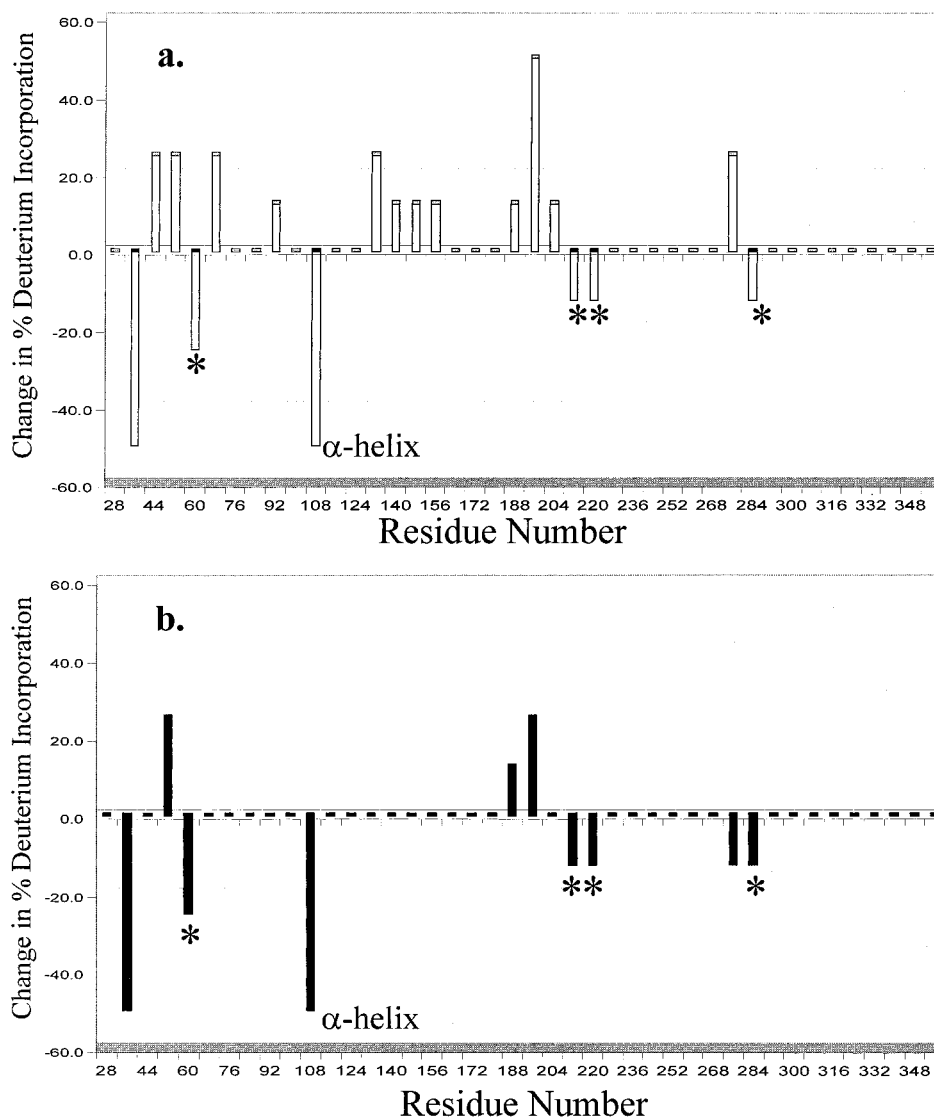


FIGURE 2: In the initial experiment, some deuterium was incorporated into free mEPG-II. From the mass spectral data, the amount of deuterium incorporated into segments of the mEPG-II sequence, approximately eight amino acids long, was deduced. The percent incorporation into each segment was calculated by dividing the number of incorporated deuterons by the number of amino acids in the peptide and multiplying by 100. Shown here are the changes in percent deuterium incorporation of mEPG-II (a) caused by the presence of (GalA)<sub>8</sub> and (b) caused by the presence of both (GalA)<sub>8</sub> and PGIP. Asterisks indicate regions in the binding cleft that are protected by the substrate.

increase in the level of deuterium incorporation as a result of ligand binding far from the region of initial interest (the binding cleft) may point toward a possible mechanism for the activity of EPG-II and also serves to demonstrate the value of the technique.

PDEs often have lysine residues that stabilize the carboxylates on the carbohydrate substrate (46–50). The  $\alpha$ -helix at Asp<sub>110</sub>–Trp<sub>114</sub> is directly below a loop that hangs predominantly over the cleft. It should be noted that there is a similar loop on the opposite side of the cleft. There are a total of four lysine residues on the two overhanging loops, and homology mapping has revealed that at least one lysine is conserved within the family of EPGs (Figure 3a). If these two overhanging loops are required to “lean” into the cleft to allow the lysines to interact with and stabilize the substrate, then much like a spring, EPG-II may flex the  $\beta$ -sheets on the underside of the barrel to accommodate the necessary movement. Modeling of this system is underway to evaluate this possibility. The flexing may, alternatively, be due to entropic considerations. The complex is at a lower-entropy

state than the unbound EPG-II if no conformational changes occur, which is unfavorable with respect to the Gibbs free energy. This phenomenon has been discussed previously in the literature (51). NMR relaxation experiments have indicated that while protein flexibility typically decreases with binding of a ligand, in a few cases it has been noted to increase (51). Our system seems to fall into this latter class. Major urinary protein I (MUP-I) from mouse has been shown to increase in flexibility when bound to the pheromone 2-sec-butyl-4,5-dihydrothiazole. MUP-I, similar to EPG-II, is almost entirely comprised of  $\beta$ -sheets, and the increase in flexibility was seen throughout the  $\beta$ -barrel upon binding of the pheromone. It has been suggested that increases in protein backbone flexibility would likely be associated with a corresponding decrease in the flexibility of another region (51). Both of these conditions are observed in the mEPG-II–homogalacturonan complex.

The mEPG-II–homogalacturonan complex was also analyzed by UV fluorescence. Tryptophan and tyrosine residues can both fluoresce. The fluorescence signal can be quenched

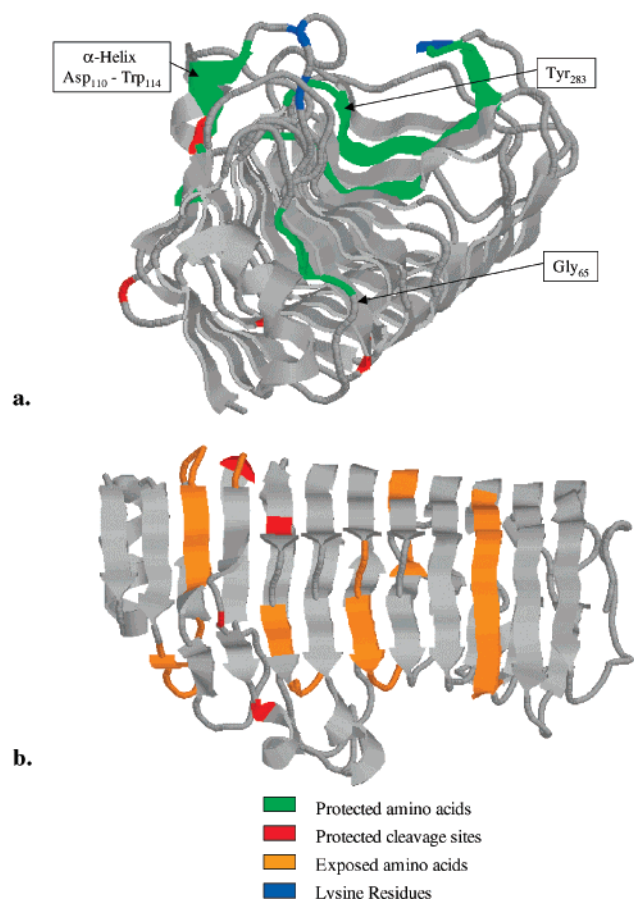


FIGURE 3: Crystal structure of EPG-II from *A. niger* from the (a) top and (b) bottom. Amino acids in the binding cleft that were protected from exchange by substrate binding are shown in green (a). Amino acids of  $\beta$ -pleated sheets that were exposed to exchange due to substrate binding are shown in gold (b). The helix at Asp<sub>110</sub> is labeled and shown in green (a). The four residues that were protected from pepsin hydrolysis by PGIP binding are shown in red (19).

by interactions with the solvent, neighboring amino acids, and other prosthetic groups. These various neighbors can allow alternatives to fluorescence as a pathway for relaxation, i.e., internal conversion. Therefore, general changes in protein structure that perturb the microenvironment of fluorescing residues may be detected if a noticeable change in fluorescence intensity is observed (52, 53). While the protein was excited at 290 nm, such that only the tryptophans will fluoresce, an increase of intensity was observed in the presence of the oligosaccharide (Figure 4). Of the seven tryptophans, five are on the underside far from the binding cleft. The remaining two are on the loop above the D<sub>110</sub>  $\alpha$ -helix. The tryptophans that are most responsible for the change in fluorescence cannot be fully determined, but the change in fluorescence is consistent with the structural changes defined by the amide exchange data.

**EPG-II–PGIP–Homogalacturonan Complex.** The PGIP proved to be highly resistant to proteolysis. The reason for this is unknown, but may be related to the LRR structure of the protein (15, 16). This resistance proved to be extremely advantageous to the experiments described here for two reasons. First, the mass spectra of the mEPG-II peptides were not further complicated by the appearance of PGIP peptides. Second, the intact PGIP blocked regions of mEPG-II from

pepsin digestion, allowing the location on mEPG-II of the mEPG-II–PGIP interaction to be probed by differential peptide mapping. When the mEPG-II peptides are compared, four residues [Glu<sub>95</sub>, Gly<sub>104</sub>, Asp<sub>110</sub>, and Ile<sub>139</sub> (Figure 3b)] that had consistently been cleavage sites in the mEPG-II and mEPG-II–homogalacturonan samples were now protected from pepsin by the presence of PGIP. Quite conclusively, the four residues lie closely together around the underside of the barrel near the region of the D<sub>110</sub>  $\alpha$ -helix, opposite the binding site and clearly pointed to the location where the inhibitor was interacting with mEPG-II. This positioning is perfectly consistent with the other experimental results and with reports of PGIP acting as a noncompetitive inhibitor (14).

The presence of the PGIP also resulted in a marked change in the pattern of deuterium incorporation in the mEPG-II–substrate complex. As described above, deuterium was not incorporated into the  $\beta$ -sheets in free mEPG-II. In the presence of substrate, the  $\beta$ -sheets are apparently disrupted, allowing deuterium to be incorporated along the underside of the barrel indicated by upward-pointing bars in Figure 2a. When PGIP is added to form the mEPG-II–PGIP–homogalacturonan complex, most of the upward-pointing bars are eliminated, indicating that the level of deuterium incorporation into the  $\beta$ -sheets along the underside of the mEPG-II is greatly reduced (Figure 2b). There are at least two explanations for this protection from exchange. Because the PGIP is binding within this region, it is certainly directly protecting some of these residues from the solvent. In addition, this interaction may be preventing disruption of  $\beta$ -sheets not directly contacted by the PGIP.

The incorporation around the Asp<sub>110</sub>  $\alpha$ -helix is also significant. In free mEPG-II, deuterium is incorporated into the  $\alpha$ -helix, implying that the  $\alpha$ -helix must be only loosely formed despite the appearance of a tightly wound helix in the crystal structure. Subsequently, in the presence of a substrate, no deuterium is incorporated, implying that the  $\alpha$ -helix may be forming more tightly during the binding process. In the presence of both the substrate and inhibitor, we also find deuterium is not incorporated into the  $\alpha$ -helix indicated by a downward bar in Figure 2b. The inhibitor may be unable to prevent the tightening of the helix in the presence of the substrate, indicating that flexing of the backbone and tightening of the  $\alpha$ -helix are not necessarily concerted or even related. Another possibility is that the PGIP is binding near and directly protecting the helix from exchange.

The amino acids in the binding cleft which are protected from exchange by substrate binding remain protected in the presence of the inhibitor, providing strong evidence that a stable tertiary system, the mEPG-II–PGIP–homogalacturonan complex, has been formed. For additional verification, fluorescence spectra of mEPG-II–PGIP and mEPG-II–PGIP–homogalacturonan complexes were generated and compared. As shown in Figure 4, the spectra are different, implying that the inhibitor is not simply displacing the substrate. As described above, PGIP has for some hosts been demonstrated to be a noncompetitive inhibitor, slowing the hydrolysis process without preventing the binding of substrate (14). In contrast to our amide exchange and fluorescence data, a recent article (54) has found evidence for competitive inhibition for the *P. vulgaris* PGIP–*Fusarium*

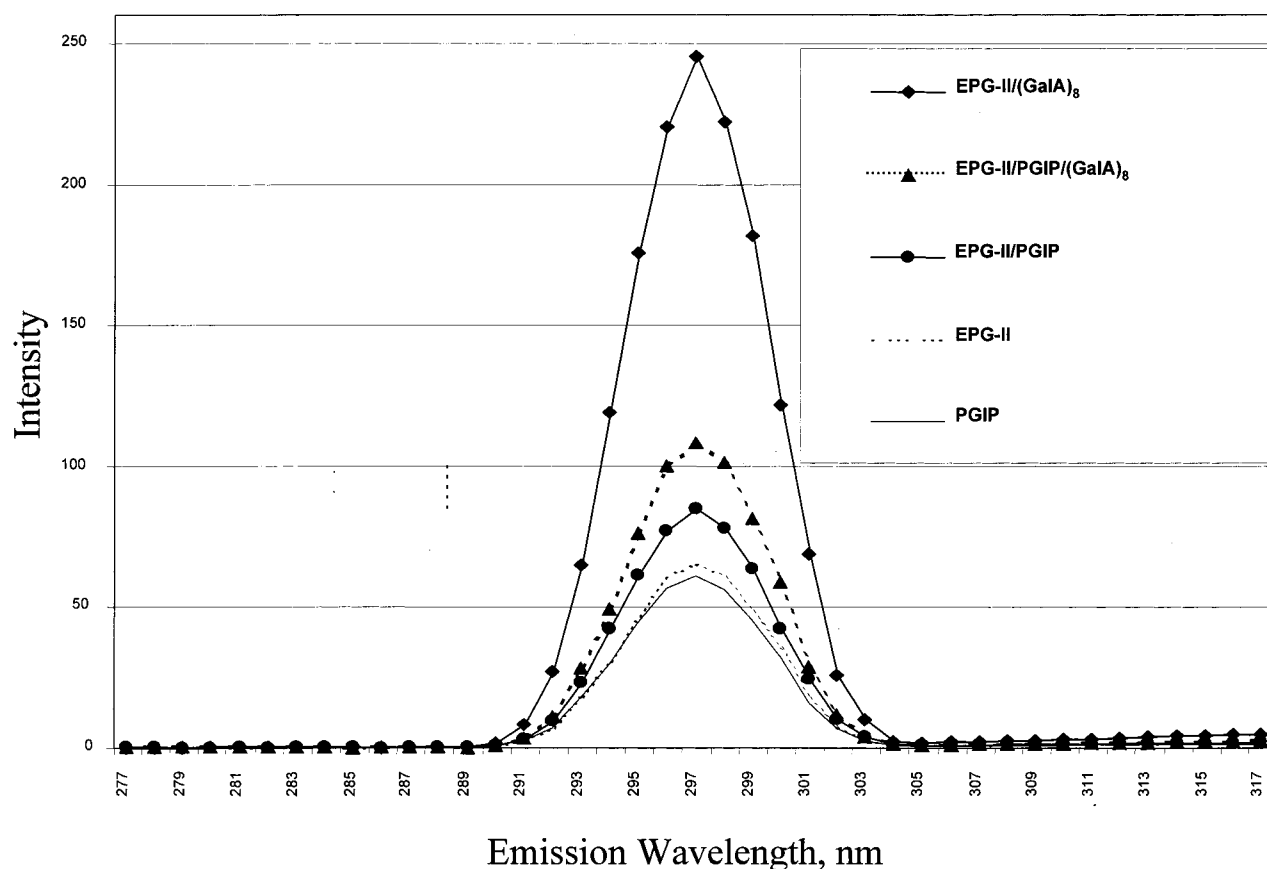


FIGURE 4: Fluorescence spectra of various mEPG-II and PGIP complexes. The emission spectra were recorded at 290 nm.

*moniliforme* EPG pairing. While this makes a general consensus more difficult, it emphasizes the complex nature of these systems and the need for independent evaluation of each enzyme–inhibitor pair.

The fluorescence experiment also provided additional evidence for conformational changes within the mEPG-II–PGIP–homogalacturonan system. Figure 4 shows the fluorescence of free mEPG-II, the mEPG-II–homogalacturonan complex, and the mEPG-II–PGIP–homogalacturonan complex. The fluorescence, as described earlier, increases dramatically with the binding of the substrate. The presence of the PGIP has a remarkable effect on the level of fluorescence, lowering it almost back to the level of free mEPG-II. The fluorescence data imply that the PGIP may be able to prevent at least some of the conformational changes caused by the presence of the substrate. The amide exchange-MS experiments have pointed out two conformational changes that occur within mEPG-II when it binds to (GalA)<sub>8</sub> that may be important, a disruption of  $\beta$ -sheets in the backbone and the formation of an  $\alpha$ -helix. Therefore, an increase in fluorescence intensity corresponds to a change in the structured environment of the tryptophans. The dramatic decrease in fluorescence caused by the presence of the PGIP clearly implicates the involvement of PGIP in changing the environments of the tryptophans. The similarity between this fluorescence intensity and that of free mEPG-II suggests that the inhibitor may be restraining the conformational changes that occurred in the mEPG-II–homogalacturonan system. If the conformational change is required for substrate binding, preventing that change may allow the substrate to diffuse away from the enzyme before hydrolysis

of the glycosidic bond can occur, thus effectively inhibiting the activity of the enzyme.

## CONCLUSION

The amide exchange-MS results indicate that the presence of PGIP had a clear effect on the deuterium incorporation in comparison to the results of the mEPG-II–homogalacturonan experiments. The most significant change involved the  $\beta$ -sheets on the underside of the barrel structure. In the presence of (GalA)<sub>8</sub>, these  $\beta$ -sheets incorporated deuterium.  $\beta$ -Sheets should not incorporate deuterium because they are involved in hydrogen bonding. So, clearly, a conformational change is occurring during substrate binding, specifically, the disruption of the  $\beta$ -sheets. In the presence of PGIP, the  $\beta$ -sheets no longer incorporate deuterium, much like free mEPG-II. The results suggest that PGIP is binding to mEPG-II on the underside of the barrel and below the Asp<sub>110</sub>  $\alpha$ -helix. This location for PGIP interaction is consistent with non-competitive inhibition.

The other region of interest is the  $\alpha$ -helix near residue 110. In free mEPG-II, deuterium was incorporated into a region shown to be an  $\alpha$ -helix in the crystal structure. A likely explanation is that the  $\alpha$ -helix is not tightly formed in the free system. The deuterium incorporation is not an artifact of the procedure, as in the presence of the substrate, deuterium is no longer incorporated into the helix. Thus, the  $\alpha$ -helix may be tightening as part of the function of EPG-II binding its substrate. The PGIP appears to have no effect on the incorporation of deuterium in the  $\alpha$ -helix peptide.

The mechanistic picture that is drawn from these experiments demonstrates not only the value of the amide



exchange-MS technique but the possible complex and specific nature of EPGs and PGIPs. The apparent flexing of the EPG-II barrel, whether caused by the lysine loops bending into the cleft to interact with the acidic substrate, is a pathway that likely decreases the activation energy for homogalacturonan hydrolysis, and the noncompetitive inhibition of this conformational change by PGIP effectively slows the hydrolysis rate by maintaining a higher energy barrier for hydrolysis. Future studies will include other EPG-PGIP pairings. Only by characterizing additional complexes can general conclusions regarding polygalacturonases and polygalacturonase-inhibiting proteins begin to be made.

## REFERENCES

- O'Neill, M. A., Darvill, A. G., and Albersheim, P. (2002) Pectic Substances, in *Encyclopedia of Life Sciences*, Macmillan Reference Ltd., London (in press).
- Jones, T. M., Anderson, A. J., and Albersheim, P. (1972) Host-pathogen interactions IV, Studies on the polysaccharide-degrading enzymes secreted by *Fusarium oxysporum* f. sp. *lycopersici*, *Physiol. Plant Pathol.* 2, 153–166.
- Karr, A. L., Jr., and Albersheim, P. (1970) Polysaccharide-degrading enzymes are unable to attack plant cell walls without prior action by a "wall-modifying enzyme", *Plant Physiol.* 46, 69–80.
- Bateman, D. F., and Basham, H. G. (1976) Degradation of Plant Cell Walls and Membranes by Microbial Enzymes, in *Encyclopedia of Plant Pathology* (Heitefuss, R., and Williams, P. H., Eds.) New Series, Vol. 4, Physiological Plant Pathology, pp 316–355, Springer-Verlag, New York.
- Hahn, M. G., Bucheli, P., Cervone, F., Doares, S. H., O'Neill, R. A., Darvill, A., and Albersheim, P. (1989) The Roles of Cell Wall Constituents in Plant-Pathogen Interactions, in *Plant-Microbe Interactions. Molecular and Genetic Perspectives* (Kosuge, T., and Nester, E. W., Eds.) Vol. 3, pp 131–181, McGraw-Hill, New York.
- Cervone, F., De Lorenzo, G., Salvi, G., Bergmann, C., Hahn, M. G., Ito, Y., Darvill, A., and Albersheim, P. (1989) Release of Phytoalexin Elicitor-Active Oligogalacturonides by Microbial Pectic Enzymes, in *Signal Molecules in Plants and Plant-Microbe Interactions* (Lugtenberg, B. J. J., Ed.) NATO ASI Series, Vol. H36, pp 85–89, Springer-Verlag, Heidelberg, Germany.
- Rose, J. K. C., O'Neill, M. A., Albersheim, P., and Darvill, A. (2000) The Primary Cell Walls of Higher Plants, in *Oligosaccharides in Chemistry and Biology-A Comprehensive Handbook* (Ernst, B., Sinay, P., and Hart, G., Eds.) pp 783–808, Wiley, London.
- Darvill, A., Bergmann, C., Cervone, F., De Lorenzo, G., Ham, K.-S., Spiro, M. D., York, W. S., and Albersheim, P. (1994) Oligosaccharins involved in plant growth and host-pathogen interactions, *Biochem. Soc. Symp.* 60, 89–94.
- Cervone, F., De Lorenzo, G., Aracri, B., Bellincampi, D., Caprari, C., Devoto, A., Leckie, F., Mattei, B., Nuss, L., and Salvi, G. (1996) The PGIP (Polygalacturonase-Inhibiting Protein) Family: Extracellular Proteins Specialized for Recognition, in *Biology of Plant-Microbe Interactions* (Stacey, G., Mullin, B., and Gresshoff, P. M., Eds.) pp 93–98, International Society for Molecular Plant-Microbe Interactions, St. Paul, MN.
- Cook, B. J., Clay, R. P., Bergmann, C. W., Albersheim, P., and Darvill, A. G. (1999) Fungal polygalacturonases exhibit different substrate degradation patterns and differ in their susceptibilities to polygalacturonase inhibiting proteins, *Mol. Plant-Microbe Interact.* 12, 703–711.
- Cervone, F., Hahn, M. G., De Lorenzo, G., Darvill, A., and Albersheim, P. (1989) Host-pathogen interactions XXXIII, A plant protein converts a fungal pathogenesis factor into an elicitor of plant defense responses, *Plant Physiol.* 90, 542–548.
- Di Pietro, A., and Roncero, M. I. G. (1996) Endopolygalacturonase from *Fusarium oxysporum* f. sp. *lycopersici*: Purification, characterization, and production during infection of tomato plants, *Phytopathology* 86, 1324–1330.
- Desiderio, A., Aracri, B., Leckie, F., Mattei, B., Salvi, G., Tigelaar, H., Van Roekel, J. S. C., Baulcombe, D. C., Melchers, M. S., De Lorenzo, G., and Cervone, F. (1997) Polygalacturonase-inhibiting proteins (PGIPs) with different specificities are expressed in *Phaseolus vulgaris*, *Mol. Plant-Microbe Interact.* 10, 852–860.
- Stotz, H. U., Bishop, J. G., Bergmann, C. W., Koch, M., Albersheim, P., Darvill, A. G., and Labavitch, J. M. (2000) Identification of target amino acids that affect interactions of fungal polygalacturonases and their plant inhibitors, *Physiol. Mol. Plant Pathol.* 56, 117–130.
- Kajava, A. V. (1998) Structural diversity of leucine-rich repeat proteins, *J. Mol. Biol.* 277, 519–527.
- Leckie, F., Mattei, B., Capodicasa, C., Hemmings, A., Nuss, L., Aracri, B., De Lorenzo, G., and Cervone, F. (1999) The specificity of polygalacturonase-inhibiting protein (PGIP): a single amino acid substitution in the solvent-exposed  $\beta$ -strand/ $\beta$ -turn region of the leucine-rich repeats (LRRs) confers a new recognition capability, *EMBO J.* 18, 2352–2363.
- Stotz, H. U., Bishop, J., Bergmann, C. W., Koch, M., Albersheim, P., Darvill, A. G., and Labavitch, J. M. (1999) Evidence for divergent selection of amino acid sites in the evolution of fungal polygalacturonases and their plant inhibitors, *Physiol. Mol. Plant Pathol.* 56, 117–130.
- Pickersgill, R., Smith, D., Worboys, K., and Jenkins, J. (1998) Crystal structure of polygalacturonase from *Erwinia carotovora* ssp. *carotovora*, *J. Biol. Chem.* 273, 24660–24664.
- Van Santen, Y., Benen, J. A. E., Schroer, K.-H., Kalk, K. H., Armand, S., Visser, J., and Dijkstra, B. W. (1999) 1.68-Å Crystal structure of endopolygalacturonase II from *Aspergillus niger* and identification of active site residues by site-directed mutagenesis, *J. Biol. Chem.* 274, 30474–30480.
- Coutinho, P. M., and Henrissat, B. (1999) The Modular Structure of Cellulases and Other Carbohydrate-Active Enzymes: an Integrated Database Approach, in *Genetics Biochemistry and Ecology of Cellulose Degradation* (Ohmiya, K., Hayashi, K., Sakka, K., Kobayashi, Y., Karita, S., and Kimura, T., Eds.) pp 15–23, Uni Publishers Co., Tokyo.
- Grassin, C., and Fauquembergue, P. (1996) Application of Pectinases in Beverages, in *Pectins and Pectinases* (Visser, J., and Voragen, A. G. J., Eds.) pp 453–462, Elsevier Science B. V., Amsterdam.
- Heldt-Hansen, H. P., Kofod, L. V., Budolfsen, G., Nielsen, P. M., Hüttel, S., and Bladt, T. (1996) Application of Tailormade Pectinases, in *Pectins and Pectinases* (Visser, J., and Voragen, A. G. J., Eds.) pp 463–474, Elsevier Science B. V., Amsterdam.
- Cooper, R. M. (1995) The Mechanisms and Significance of Enzymic Degradation of Host Cell Walls by Parasites, in *Biochemical Plant Pathology* (Callow, J. A., Ed.) p 135, John Wiley and Sons Ltd., London.
- Bergmann, C. W., Cook, B., Darvill, A. G., Albersheim, P., Bellincampi, D., and Caprari, C. (1995) The Effect of Glycosylation of Endopolygalacturonases and Polygalacturonase Inhibiting Proteins on the Production of Oligogalacturonides, in *Pectins and Pectinases* (Visser, J., and Voragen, A. G. J., Eds.) pp 275–282, Elsevier Science B. V., Amsterdam.
- Thakur, B. R., Singh, R. K., and Handa, A. K. (1997) Chemistry and uses of pectin: A review, *Crit. Rev. Food Sci. Nutr.* 37, 47–73.
- Katta, V., and Chait, B. T. (1993) Hydrogen/deuterium exchange electrospray ionization mass spectrometry: a method for probing protein conformational changes in solution, *J. Am. Chem. Soc.* 115, 6317–6321.
- Zhang, Z. Q., and Smith, D. L. (1993) Determination of amide hydrogen-exchange by mass-spectrometry: a new tool for protein-structure elucidation, *Protein Sci.* 2, 522–531.
- Liu, Y. Q., and Smith, D. L. (1994) Probing high-order structure of proteins by fast-atom-bombardment mass-spectrometry, *J. Am. Soc. Mass Spectrom.* 5, 19–28.
- Satoko, A., and Takio, K. (2000) Characterization of the interface structure of enzyme-inhibitor complex by using hydrogen-deuterium exchange and electrospray ionization Fourier transform ion cyclotron resonance mass spectrometry, *Protein Sci.* 9L, 2497–2505.
- Falick, A. M., and Komives, E. A. (1998) Identification of protein-protein interfaces by decreased amide proton solvent accessibility, *Proc. Natl. Acad. Sci. U.S.A.* 95, 14705–14710.
- Farmer, T. B., and Caprioli, R. M. (1998) Determination of protein-protein interactions by matrix-assisted laser desorption/ionization mass spectrometry, *J. Mass Spectrom.* 33, 697–704.
- Ehring, H. (1999) Hydrogen exchange/electrospray ionization mass spectrometry studies of structural features of proteins and protein/protein interactions, *Anal. Biochem.* 267, 252–259.



33. Smith, D. L., and Zhang, Z. Q. (1994) Probing noncovalent structural features of proteins by mass-spectrometry, *Mass Spectrom. Rev.* 13, 411–429.
34. Smith, J. B., Liu, Y. Q., and Smith, D. L. (1996) Identification of possible regions of chaperone activity in lens alpha-crystallin, *Exp. Eye Res.* 63, 125–127.
35. Armand, S., Wagemaker, M. J. M., Sanchez-Torres, P., Kester, H. C. M., van Santen, Y., Eijksstra, B. W., Visser, J., and Benen, J. A. E. (2000) The active site topology of *Aspergillus niger* endopolygalacturonase II as studied by site-directed mutagenesis, *J. Biol. Chem.* 275, 691–696.
36. Toubart, P., Desiderio, A., Salvi, G., Cervone, F., Daroda, L., De Lorenzo, G., Bergmann, C., Darvill, A. G., and Albersheim, P. (1992) Cloning and characterization of the gene encoding the polygalacturonase-inhibiting protein (PGIP) of *Phaseolus vulgaris* L., *Plant J.* 2, 367–373.
37. King, D., Lumpkin, M., Bergmann, C., and Orlando, R. (2002) Studying protein-carbohydrate interactions by amide hydrogen/deuterium exchange mass spectrometry, *Rapid Commun. Mass Spectrom.* (in press).
38. Mandell, J. G., Baerga-Ortiz, A., Akashi, S., Takio, K., and Komives, E. A. (2001) Solvent accessibility of the thrombin-thrombomodulin interface, *J. Mol. Biol.* 306, 575–589.
39. Milne, J. S., Mayne, L., Roder, H., Wand, A. J., and Englander, S. W. (1998) Determinants of protein hydrogen exchange studied in equine cytochrome c, *Protein Sci.* 7, 739–745.
40. Benen, J. A. E., Kester, H. C. M., and Visser, J. (1999) Kinetic characterization of *Aspergillus niger* N400 endopolygalacturonases I, II, and C, *Eur. J. Biochem.* 259, 577–585.
41. Papnikolau, Y., Prag, G., Tavlak, G., Vorgias, C. E., Oppenheim, A. B., and Petratos, K. (2000) Crystal structure of chitinase a mutant E315q complexed with octa-N-acetylchitooctose (Nag)<sub>8</sub>, <http://pdb.ccdc.cam.ac.uk/oca-bin/ccpeek?id=1EHN>.
42. Scavetta, R. D., Herron, S. R., Hotchkiss, A. T., Kita, N., Keen, N. T., Benen, J. A., Kester, H. C., Visser, J., and Jurnak, F. (1999) Structure of a plant cell wall fragment complexed to pectate lyase C, *Plant Cell* 11, 1081–1092.
43. Wang, L., Lane, L. C., and Smith, D. L. (2001) Detecting structural changes in viral capsids by hydrogen exchange and mass spectrometry, *Protein Sci.* 10, 1234–1243.
44. Raschke, T. M., and Marqusee, S. (1998) Hydrogen exchange studies of protein structure, *Curr. Opin. Biotechnol.* 9, 80–86.
45. Jeng, M. F., Englander, W., Elove, G. A., Wand, A. J., and Roder, H. (1990) Structural description of acid-denatured cytochrome c by hydrogen exchange and 2D NMR, *Biochemistry* 29, 10433–10437.
46. Stotz, H. U., Bergmann, C. W., Powell, A. L. T., Contos, J. J., Albersheim, P., Darvill, A. G., and Labavitch, J. M. (1994) Structural and functional comparison of polygalacturonase inhibitor proteins from pear, tomato, and bean, Abstract from the 7th International Symposium on Molecular Plant-Microbe Interactions, Edinburgh, U.K.
47. Fromm, J. R., Hileman, R. E., Caldwell, E. E., Weilere, J. M., and Linhardt, R. J. (1997) Pattern and spacing of basic amino acids in heparin binding sites, *Arch. Biochem. Biophys.* 343, 92–100.
48. Fromm, J. R., Hileman, R. E., Caldwell, E. E. O., Weiler, J. M., and Linhardt, R. J. (1995) Differences in the interaction of heparin with arginine and lysine and the importance of these basic amino acids in the binding of heparin to acidic fibroblast growth factor, *Arch. Biochem. Biophys.* 323, 279–287.
49. Quijcho, F. A. (1986) Carbohydrate-binding proteins: tertiary structures and protein-sugar interactions, *Annu. Rev. Biochem.* 55, 287–315.
50. Monchois, V., Willemot, R. M., and Monsan, P. (1999) Glucan-sucrases: mechanism of action and structure–function relationships, *FEMS Microbiol. Rev.* 23, 131–151.
51. Zidek, L., Novotny, M. V., and Stone, M. J. (1999) Increased protein backbone conformational entropy upon hydrophobic ligand binding, *Nat. Struct. Biol.* 6, 12, 1118–1121.
52. Nichols, N. M., and Matthews, K. S. (2000) p53 Unfolding detected by CD but not by tryptophan fluorescence, *Biochem. Biophys. Res. Commun.* 288, 111–115.
53. Willard, H. H., Merriitt, L. L., Jr., Dean, J. A., and Settle, F. A. (1988) *Instrumental Methods of Analysis*, pp 197–202, Wadsworth Publishing Co., Belmont, CA.
54. Federici, L., Caprari, C., Mattei, B., Savino, C., Di Matteo, A., De Lorenzo, G., Cervone, F., and Tsernoglou, D. (2001) Structural requirements of endopolygalacturonase for the interaction with PGIP (polygalacturonase-inhibiting protein), *Proc. Natl. Acad. Sci. U.S.A.* 98, 13425–13430.

BI020119F